# Modeling the Electronic Behavior of $\gamma$-$LiV_2O_5$: A Microscopic Study

Roser Valentí,[1] T. Saha-Dasgupta,[2] J. V. Alvarez,[1] K. Požgajčić,[1] and Claudius Gros[1]

[1]*Fakultät 7, Theoretische Physik, University of the Saarland, 66041 Saarbrücken, Germany*

[2]*Bose National Centre for Basic Sciences, JD Block, Sector 3, Salt Lake City, Kolkata 700098, India*

(Received 18 January 2001)

We determine the electronic structure of the one-dimensional spin-$\frac{1}{2}$ Heisenberg compound $\gamma$-$LiV_2O_5$, which has two inequivalent vanadium ions, V(1) and V(2), via density-functional calculations. We find a relative V(1)-V(2) charge ordering of roughly 70:30. We discuss the influence of the charge ordering on the electronic structure and the magnetic behavior. We give estimates of the basic hopping matrix elements and compare with the most studied $\alpha'$-$NaV_2O_5$.

DOI: 10.1103/PhysRevLett.86.5381 PACS numbers: 75.30.Gw, 75.10.Jm, 78.30.–j

Low-dimensional transition metal compounds have been intensively studied in the past few years. Among those, the quarter-filled ladder compound [1,2] $\alpha'$-$NaV_2O_5$ has become a model substance for the study of spin-charge and orbital coupling. The coupling between spin and orbital ordering is a central issue in the somewhat more complex colossal magnetoresistance (CMR) materials [3]; the advantage of $\alpha'$-$NaV_2O_5$ as a model compound is the spatial separation of the two $d_{xy}$ orbitals onto two spatially separated $V^{4.5+}$ sites, arranged in ladders. These two orbitals undergo a charge-order transition [4] at $T_c = 34$ K with $2V^{4.5+} \rightarrow V^{4+} + V^{5+}$. Simultaneously to the charge order and the respective lattice distortions [5], a spin gap [6] opens, indicating substantial spin-charge coupling in this compound. The physics of this transition is being studied intensively [7,8].

A much less studied, though not less intriguing, system belonging to the same vanadium oxide family is $\gamma$-$LiV_2O_5$. Susceptibility measurements [9], as well as NMR experiments [10], on this compound suggest a one-dimensional spin-$\frac{1}{2}$ Heisenberg-like behavior and there is no indication of a phase transition at lower temperatures. To our knowledge, there is no microscopic study of the electronic structure of this material discussing the magnetic interactions responsible for such behavior. We present here a density-functional analysis (DFT) of this system and calculate the possible exchange matrix elements via the linear muffin-tin orbital (LMTO) based downfolding method [11] and a tight-binding model.

$\gamma$-$LiV_2O_5$ offers the possibility, due to its close relation to $\alpha'$-$NaV_2O_5$, to study the influence of charge ordering on the electronic structure. In particular, this opens the question on how far the charge ordering and the corresponding crystallographic distortions alter the magnetic interactions. We discuss several possible scenarios compatible with the experimental susceptibility for $\gamma$-$LiV_2O_5$ for the underlying magnetic model: (i) a zigzag chain model of V(1) ions, (ii) a double-chain model of V(1) ions, and (iii) an asymmetric quarter-filled ladder model.

*Crystal structure.*—$\gamma$-$LiV_2O_5$ has a layered structure of $VO_5$ square pyramids with lithium ions between the layers. It crystallizes [12] in the orthorhombic centrosymmetric space group $D_{2h}^{16}$-*Pnma* and has two crystallographic inequivalent vanadium sites, V(1) and V(2), which form two different zigzag chains running along the $y$ axis. Within the layers, $V(1)O_5$ zigzag chains are linked to $V(2)O_5$ zigzag chains by corner sharing via the bridging O(1). The existence of two types of V sites has been also verified by NMR experiments [13].

In Fig. 1 we show the crystal structure of $\gamma$-$LiV_2O_5$ and $\alpha'$-$NaV_2O_5$ projected on the $xz$ plane. The angle between the basal plane of the (nearly) square $V(1)O_5/V(2)O_5$ pyramids and the $x$ axis is about $+30°/-30°$, respectively, for $\gamma$-$LiV_2O_5$. The basal plane of the $VO_5$ pyramids in $\alpha'$-$NaV_2O_5$ is, on the other hand, nearly parallel to the $x$ axis. Note that the $VO_5$ square pyramids are oriented along $x$ as down-down-up-up in $\alpha'$-$NaV_2O_5$, while in $\gamma$-$LiV_2O_5$ the orientation is down-up-down-up.

From the structural analysis it has been proposed [12] that the oxidations of V(1) and V(2) are, respectively, $V^{4+}$ and $V^{5+}$. The temperature dependence of the susceptibility $\chi(T)$ follows that of a one-dimensional spin-$\frac{1}{2}$ Heisenberg model with an exchange interaction of $J_{\text{exp}} = 308$ K and a

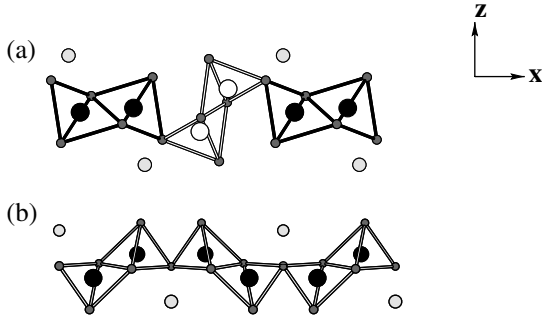


FIG. 1. Crystal structure of (a) $\gamma$-$LiV_2O_5$ and (b) $\alpha'$-$NaV_2O_5$ projected in the $(xz)$ plane. For $\gamma$-$LiV_2O_5$ the $(xz)$ cut through one of the two equivalent $xy$ planes is shown here. The large circles are the V ions, black and white for V(1) and V(2), respectively, in $\gamma$-$LiV_2O_5$, and black for $\alpha'$-$NaV_2O_5$. The oxygens are represented by the smaller circles. The alkali ions (Li, Na), shown by grey circles, are located in between the planes, close to the bridging oxygens.

  

gyromagnetic factor $g = 1.8$ [9]. Note that depending on the magnitude of the exchange couplings, $J_1$—between V(1) ions in edge-shared pyramids—and $J_b$—between V(1) ions in corner-shared pyramids—along $y$ the system can be treated as Heisenberg zigzag chains ($J_1 \gg J_b$) or as Heisenberg double-linear chains ($J_1 \ll J_b$); compare with Fig. 2.

A third possible interpretation of the nature of $\gamma$-$LiV_2O_5$ compatible with the experimental susceptibility relies on the possibility of a *partially* charge-ordered system, i.e., V(1) sites somewhat closer to $V^{4+}$ oxidation and V(2) sites closer to $V^{5+}$ oxidation. A picture of an asymmetric ladder with one electron per V(1)-O-V(2) rung would then describe the system in analogy to $\alpha'$-$NaV_2O_5$ where the magnetic interactions among the constituent ladders are weak [14]. In the following, we investigate these three scenarios.

*Band structure.*—We have calculated the energy bands (see Fig. 3) of $\gamma$-$LiV_2O_5$ within DFT by employing the full-potential linearized augmented plane wave code WIEN97 [15] and by LMTO [16] based on the Stuttgart TBLMTO-47 code. We find complete agreement in between these two calculations.

The overall band picture for $\gamma$-$LiV_2O_5$ (Fig. 3) is similar to that of $\alpha'$-$NaV_2O_5$ [1]. The V-3$d$ states give the predominant contribution to the bands at the Fermi level and up to $\approx$4 eV above it. The lower valence bands are mainly O-2$p$ states and are separated by a gap of $\approx$2.2 eV from the bottom of the V-3$d$ bands. There is a nonequivalent contribution from the two types of V sites, V(1) and V(2). The four lowest-lying 3$d$ bands at the Fermi level are half filled [17] and are made up predominantly of V(1)-3$d$ and of V(2)-3$d$ states in the ratio $p(1)/p(2) \approx 2{:}1$ and 3:1 depending on the $k$ values. The next four bands less than 1 eV above the Fermi level also exhibit a mixture of V(1)-3$d$ and V(2)-3$d$ character.

The vanadium bands at the Fermi level are of $d_{xy}$ symmetry (global symmetry) with a certain admixture with the $d_{yz}$ state due to the rotation of the basal plane of the $V(1/2)O_5$ pyramids with respect to the $x$ axis (see Fig. 1). The degree of admixture for both vanadium types is such that the respective V-3$d$ orbitals point—as in $\alpha'$-$NaV_2O_5$ [1]—roughly towards the bridging oxygens. In this sense, one can regard the electronic active V(1)-3$d$ and V(2)-3$d$ orbitals as $d_{xy}$ orbitals rotated around the $y$ axis by angles $\varphi_1 = 35°$ and $\varphi_2 = -28°$, respectively (see Fig. 4).

The most notable difference between the band structure of $\gamma$-$LiV_2O_5$ and $\alpha'$-$NaV_2O_5$ is the band splitting at the $X$ and $T$ points in $\gamma$-$LiV_2O_5$, which is absent in $\alpha'$-$NaV_2O_5$. This splitting is due to the existence of two different V sites in $\gamma$-$LiV_2O_5$ as we see in the next paragraph. The fact that this splitting is big, close to the overall bandwidth, indicates already that the microscopic parameters associated with the V(1) and V(2) sites must differ substantially.

Also note that the splitting of the bands at the Fermi level due to the existence of two $xy$ planes in the crystallographic unit cell of $\gamma$-$LiV_2O_5$ is small and does not occur along the path $Z$-$U$-$R$-$T$-$Z$. We concentrate upon the discussion of the in-plane dispersion in what follows.

*Microscopic parameters.*—In order to determine the microscopic model appropriate for $\gamma$-$LiV_2O_5$ we have analyzed the band structure shown in Fig. 3 by a (minimal) tight-binding model with one orbital per vanadium site, which generalizes the tight-binding model appropriate

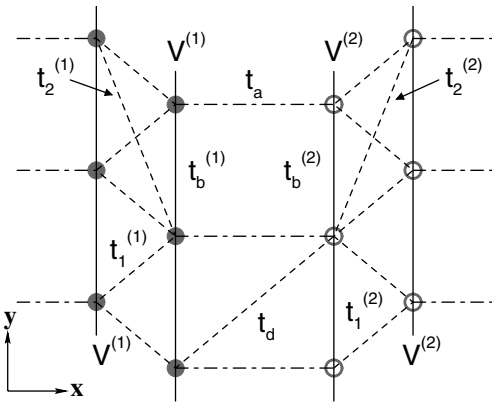


FIG. 2. Hopping parameters used for the tight-binding model for $\gamma$-$LiV_2O_5$. The arrangement of the V ions in an $xy$ plane is topologically identical to the one in $\alpha'$-$NaV_2O_5$; i.e., they form a Trellis lattice. The $t_d$ and the $t_2^{(1/2)}$ are shown only partially. Not shown are the on site energies $\pm\varepsilon_0$ of the $V(1/2)$ sites.

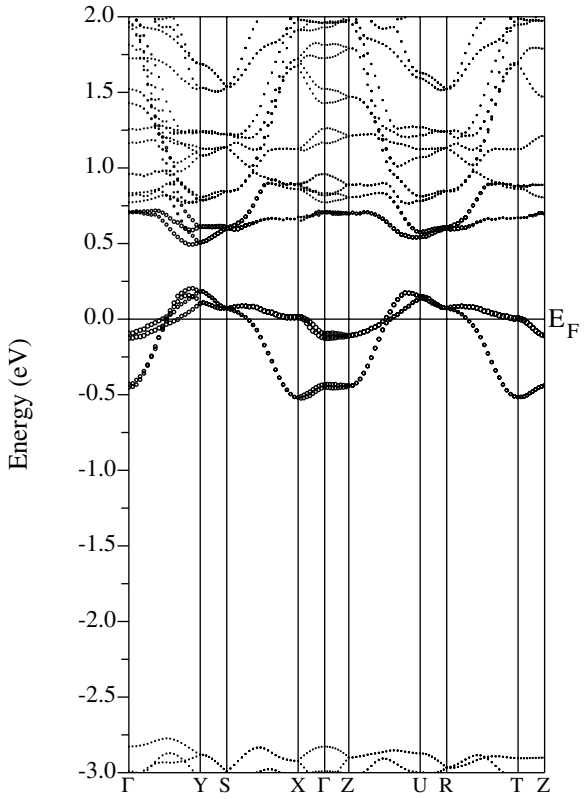


FIG. 3. LDA results for $LiV_2O_5$. The path is along $\Gamma = (0,0,0)$, $Y = (0,\pi,0)$, $S = (\pi,\pi,0)$, $X = (\pi,0,0)$, $\Gamma$, $Z = (0,0,\pi)$, $U = (0,\pi,\pi)$, $R = (\pi,\pi,\pi)$, $T = (\pi,0,\pi)$, $Z$. The V(1)-3$d_{xy}$ character of the bands is shown with bigger circles.

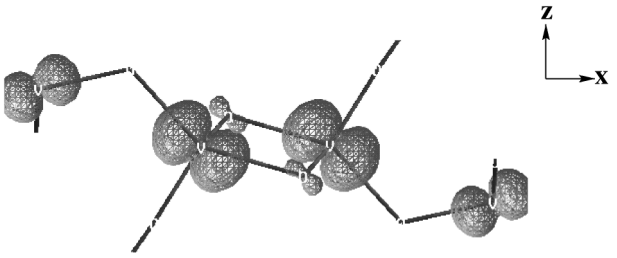


FIG. 4. Electron density of the V-3$d$ bands seen in a ($xz$) cut. Shown is the isoline 0.05 $e/\text{Å}^3$. The bigger lobes correspond to V(1)-3$d$ orbitals and the smaller ones to V(2)-3$d$ orbitals. Note that the tilted orbitals point towards the bridging oxygens (compare with Fig. 1).

for $\alpha'$-$NaV_2O_5$ to the case of two different V sites. A straightforward fit, e.g., by least squares, is not possible since the lower unoccupied V bands (roughly in between 0.5−1.0 eV) are strongly hybridized with the O-$p$ orbitals and in order to describe the low-energy physics of this system these bands should also be considered.

In recent years [11], a new version of the LMTO method has been proposed and implemented which has proved to be powerful in providing an effective orbital representation of the system by integrating out the higher degrees of freedom using the so-called downfolding technique. The usefulness of the method lies in taking into account proper renormalization effects. However, the Fourier transform of the downfolded Hamiltonian to extract the tight-binding parameters results in long-ranged hopping matrix elements.

We have therefore considered a combination of both methods. We use only the short-ranged hopping matrix elements (see Fig. 2) provided by the downfolding procedure as an input for the tight-binding model. These matrix elements are then optimized to reproduce the behavior of the *ab initio* bands near the Fermi level. The result and the parameters (apart from an overall constant energy) of the optimal fit are shown in Fig. 5.

From the relative weight between the V(1) and the V(2) contributions near the Fermi level, $p(1)/p(2)$, we learn that there must be a substantial on-site energy $\pm\epsilon_0$ for the $V(1/2)$ orbitals, respectively. We find $\epsilon_0 = 0.15$ eV. The rung-hopping matrix element $t_a$ may be expected, on the other hand, to be quite close to the one obtained for $\alpha'$-$NaV_2O_5$ [18] since the large bending angle V(1)-O(1)-V(2) should not substantially affect the $\pi$ bonding via the O(1)-$p_y$ orbital. Indeed, we find $t_a = 0.35$ eV. We can check whether our estimates for $\epsilon_0$ and $t_a$ lead to the correct V(1)-V(2) charge ordering. By diagonalizing a simple two-site rung model we find the relation

$$\frac{e_0}{t_a} = \frac{p(2) - p(1)}{2\sqrt{p(1)p(2)}}, \tag{1}$$

which yields $p(1)/p(2) = 2.3$ for $e_0/t_a = 0.15/0.35$, i.e., $p(1) \approx 0.7$ and $p(2) \approx 0.3$, in agreement with the DFT results.

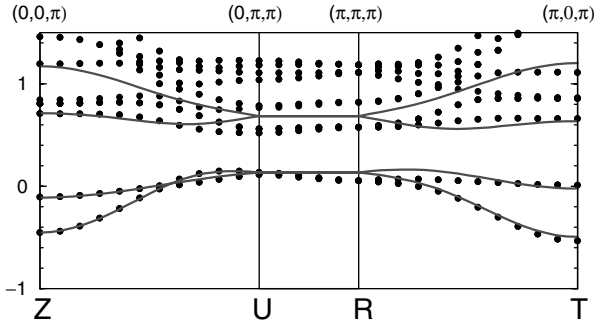


FIG. 5. Comparison of the tight-binding fit (solid lines) with the DFT bands (filled circles). The parameters used (see Fig. 2) are (in eV) $\epsilon_0 = 0.15$, $t_a = 0.35$, $t_d = 0.10$, $t_b^{(1)} = -0.06$, $t_b^{(2)} = 0.02$, $t_1^{(1)} = -0.18$, $t_2^{(1)} = -0.05$, $t_1^{(2)} = 0.05$, and $t_2^{(2)} = -0.02$.

We note next that the crossing along $\Gamma$-$Y$ and $Z$-$U$, respectively, can be described (within a V model) only by a considerable $t_2^{(1/2)}$, as it has been noted previously [1]. Recently Yaresko *et al.* [19] have discussed that this matrix element arises naturally when one integrates out the coupling between two leg oxygens of two adjacent edge-sharing $VO_5$ pyramids. Our results $t_2^{(1)} = -0.05$ eV and $t_2^{(2)} = -0.02$ eV are close to the values obtained for $\alpha'$-$NaV_2O_5$ [18].

A substantial diagonal hopping matrix element $t_d$ is needed in order to explain the fact that the dispersion along $\Gamma$-$Y$ of the lower four V bands has an opposite behavior with respect to the upper four V bands [20], as has been pointed out independently for $\alpha'$-$NaV_2O_5$ by Yaresko *et al.* [19]. The substantial contribution of $t_d = 0.10$ eV can be explained by effective V-O-O-V exchange paths [19,21]. The hopping matrix element along the V(1) leg, $t_b^{(1)} = -0.06$ eV has a similar value to the one for $\alpha'$-$NaV_2O_5$, though the sign of the effective V(2)-leg hopping parameter, $t_b^{(2)} = 0.02$ eV, is opposite to the expected one.

The result for $t_1^{(2)} = 0.05$ eV might have been expected since its corresponding value for $\alpha'$-$NaV_2O_5$ is small [18]. The result $t_1^{(1)} = -0.18$ eV is, on the other hand, substantially larger and needs some explanation. In terms of the band structure, $t_1^{(1)}$ is determined predominantly by the large splitting of the V-$d$ bands [22] at $X$ and $T$ (see Figs. 3 and 5). Also, it has been noted previously [1,2] in the context of $\alpha'$-$NaV_2O_5$ that the bare two-center Slater-Koster matrix elements contributing to $t_1$ can be as large as −0.3 eV. The effective $t_1$ is reduced from the bare two-center matrix element by the rotation of the V-3$d$ orbitals about the crystallographic $y$ axis and by interference from three-center terms [1,21]. The contribution from V-O-V exchange paths depends strongly on the relative positions of the three atoms. We have performed for $\gamma$-$LiV_2O_5$ a Slater-Koster analysis and found that due to interference effects in between the respective $dd\sigma$ and $dd\pi$ contributions, the V(2)-V(2) matrix element

contributing to $t_1^{(2)}$ is smaller than the V(1)-V(1) matrix element contributing to $t_1^{(1)}$. In addition, the exchange along V(1)-O(4)-V(1) contributing to $t_1^{(1)}$ was found to be substantially larger than the exchange V(2)-O(5)-V(2) contributing to $t_1^{(2)}$. The particular V-O-V distances and angles lead therefore to different $t_1^{(1)}$ and $t_1^{(2)}$.

*Microscopic model.*—The microscopic model corresponding to the results shown in Fig. 5 is that of a spin-$\frac{1}{2}$ antiferromagnetic Heisenberg chain where the magnetic moments are associated dominantly with the sites of the V(1) ions in $\gamma$-$LiV_2O_5$; the contribution is $p(1) \approx 0.7$. The contribution of about $p(2) \approx 0.3$ of the V(2) to the magnetic moment on a $V(2) - O(1) - V(1)$ rung has nevertheless important consequences for the underlying microscopic model. For negligible values of $p(2)$ the microscopic model could be considered as that of a zigzag chain with a $J \sim 4\frac{(t_1^{(1)})^2}{U}$ since $t_b^{(1)} = -0.06$ eV is smaller than $t_1^{(1)} \approx -0.18$ eV. In the presence of a non-negligible value of $p(2)$ the effective hopping matrix element $t_b^{(\mathrm{eff})}$ in between two asymmetric rung states along $b$ is

$$t_b^{(\mathrm{eff})} = p(1)t_b^{(1)} + p(2)t_b^{(2)} - 2\sqrt{p(1)p(2)}\,t_d \approx -0.127 \text{ eV},$$

suggesting an asymmetric ladder model. Then, using the expression $J_b = 2\frac{(t_b^{(\mathrm{eff})})^2}{E_c}$, and assuming that the charge-transfer gap is $E_c \approx 0.7$ eV as in $\alpha'$-$NaV_2O_5$ [23] the exchange integral is $J_b \approx 540$ K which overestimates the experimental value $J_{\mathrm{exp}} = 308$ K. The degree of charge ordering has therefore a substantial influence on the nature of the magnetic couplings [24].

*Conclusions.*—We have presented an analysis of DFT band-structure calculations for $\gamma$-$LiV_2O_5$. We find that the degree of charge ordering has a substantial influence on the nature of the magnetic state. Our results indicate incomplete charge ordering and $\gamma$-$LiV_2O_5$ could in this case be viewed as a spin-$\frac{1}{2}$ asymmetric quarter-filled ladder compound. This model would explain the spin wave excitation spectrum obtained by inelastic neutron scattering experiments [25]. Finally, we observe that small distortions in the lattice may have substantial effects on the interladder V-V hopping matrix element $t_1$.

This work was partially supported by the DFG. One of us (R. V.) thanks C. O. Rodriguez for helpful advice regarding the WIEN97 code and A. Kokalj for providing the graphics XCRYSDEN code.

[1] H. Smolinski, C. Gros, W. Weber, U. Peuchert, G. Roth, M. Weiden, and C. Geibel, Phys. Rev. Lett. **80**, 5164 (1998).
[2] P. Horsch and F. Mack, Eur. Phys. J. B **5**, 367 (1998).
[3] For a review, see *Colossal Magnetoresistance, Charge Ordering and Related Properties of Manganites Oxides,* edited by C. N. R. Rao and B. Raveau (World Scientific, Singapore, 1998).
[4] T. Ohama, H. Yasuoka, M. Isobe, and Y. Ueda, Phys. Rev. B **59**, 3299 (1999).
[5] See, for instance, J. Lüdecke, A. Jobst, S. van Smaalen, E. Morre, C. Geibel, and H.-G. Krane, Phys. Rev. Lett. **82**, 3633 (1999); J. L. de Boer, A. M. Meetsma, J. Baas, and T. T. M. Palstra, Phys. Rev. Lett. **84**, 3962 (2000).
[6] M. Isobe and Y. Ueda, J. Phys. Soc. Jpn. **65**, 1178 (1996).
[7] C. Gros, R. Valentí, J. V. Alvarez, K. Hamacher, and W. Wenzel, Phys. Rev. B **62**, R14 617 (2000); S. Trebst and A. Sengupta, Phys. Rev. B **62**, R14 613 (2000); A. Honecker and W. Brenig, Phys. Rev. B, **63**, 144 416 (2001).
[8] A. Bernert, T. Chatterji, P. Thalmeier, and P. Fulde, cond-mat/0012327.
[9] M. Isobe and Y. Ueda, J. Phys. Soc. Jpn. **65**, 3142 (1996).
[10] N. Fujiwara, H. Yasuoka, M. Isobe, Y. Ueda, and S. Maegawa, Phys. Rev. B **55**, R11 945 (1997).
[11] See O. K. Andersen and T. Saha-Dasgupta, Phys. Rev. B **62**, R16 219 (2000), and references therein.
[12] J. Galy and A. Hardy, Acta Crystallogr. **19**, 432 (1955); D. N. Anderson and R. D. Willett, Acta Crystallogr. B **27**, 1476 (1971).
[13] N. Fujiwara, H. Yasuoka, M. Isobe, and Y. Ueda, Phys. Rev. B **58**, 11 134 (1998).
[14] C. Gros and R. Valentí, Phys. Rev. Lett. **82**, 976 (1999).
[15] P. Blaha, K. Schwarz, and J. Luitz, WIEN97, *A Full Potential Linearized Augmented Plane Wave Package for Calculating Crystal Properties* (Karlheinz Schwarz, Technical University of Wien, Vienna, 1999), ISBN 3-9501031-0-4; updated version of P. Blaha, K. Schwarz, P. Sorantin, and S. B. Trickey, Comput. Phys. Commun. **59**, 399 (1990).
[16] O. K. Andersen, Phys. Rev. B **12**, 3060 (1975).
[17] Note that the unit cell of $LiV_2O_5$ corresponds to four formula units.
[18] The tight-binding parameters for $\alpha'$-$NaV_2O_5$ are [1,19,20] $t_a = 0.375$ eV, $t_d = 0.095$ eV, $t_b = -0.08$ eV, $t_2 = -0.055$ eV. We have reanalyzed the DFT band structure of $NaV_2O_2$ and found that the effective $t_1$ is very small.
[19] A. N. Yaresko, V. N. Antonov, H. Eschrig, P. Thalmeier, and P. Fulde, Phys. Rev. B **62**, 15 538 (2000).
[20] The dispersion of the antibonding/bonding V bands in $\alpha'$-$NaV_2O_5$ is $\pm t_a + 2(t_b \pm t_d)\cos(k_y)$. In order to obtain an opposite dispersion [1,18] one needs $t_d > |t_b|$. The bandwidth 0.7 eV $\approx 4|t_b - t_d|$ of the bonding orbital and the smaller bandwidth $\approx$0.1 eV of the antibonding orbital yield then $t_d \approx 0.095$ eV and $t_b \approx -0.08$ eV.
[21] H. Smolinski, Ph.D. thesis, Dortmund University, Dortmund, 1998.
[22] For general parameters the tight-binding equation cannot be solved analytically but certain limiting cases can be studied. As an illustration, we note that for $t_1^{(1)} = t_1^{(2)} = t_1$, $t_b^{(2)} = -t_b^{(1)}$, and $\epsilon_0^{(2)} = \epsilon_0^{(1)}$ the dispersion of the antibonding/bonding bands at $X$ and $T$ in $\gamma$-$LiV_2O_5$ is given by $\lambda^2 = [\epsilon_0 + (t_b^{(1)} - t_b^{(2)}) \pm 2t_1]^2 + (t_a + 2t_d)^2$.
[23] D. Smirnov *et al.,* Phys. Rev. B **57**, R11 035 (1998).
[24] Contributions from intermediate singlet and intermediate triplet states [2] to the interchain magnetic exchange $J_a$ nearly cancel even for relatively large values for $t_1^{(1)}$, leading to an effective small interladder exchange.
[25] Y. Takeo *et al.,* J. Phys. Chem. Solids **60**, 1145 (1999).